

The LkH α 101 Cluster

Sean M. Andrews and Scott J. Wolk

Harvard-Smithsonian Center for Astrophysics
60 Garden Street, Cambridge, MA, 02138, USA

Abstract. In the infrared, the heavily reddened LkH α 101 is one of the brightest young stars in the sky. Situated just north of the Taurus-Auriga complex in the L1482 dark cloud, it appears to be an early B-type star that has been serendipitously exposed during a rarely observed stage of early evolution, revealing a remarkable spectrum and a directly-imaged circumstellar disk. While detailed studies of this star and its circumstellar environment have become increasingly sophisticated in the 50 years since Herbig (1956) first pointed it out, the true nature of the object still remains a mystery. Recent work has renewed focus on the young cluster of stars surrounding LkH α 101, and what it can tell us about the enigmatic source at its center (e.g., massive star formation timescales, clustered formation mechanisms). This latter effort certainly deserves more intensive study. We describe the current knowledge of this region and point out interesting work that could be done in the future.

1. Introduction

In a generalized sense, there are three distinct types of young star clusters: (a) high-mass star-forming regions with an associated extensive network of low-mass stars (e.g., Orion); (b) quiescent environments that host low-mass star formation exclusively (e.g., Taurus-Auriga); and (c) smaller clusters of low-mass stars surrounding one or a few A/B stars. Naturally, there is a continuum of such types, and the picture is not quite so simple. However, an important goal in this line of research is to generally understand the differences and commonalities between these cluster types in an effort to better explain the various clustered modes of star formation and their consequences. The LkH α 101 cluster is an interesting example of the (c) type; a handful of B stars and a hundred or more low-mass stars with a dominant source (LkH α 101) at the center. The remarkable central source and apparent young age for the cluster indicate that we have been afforded a fortuitous opportunity to investigate this formation mode at a very early time. In this chapter, we highlight various studies of the LkH α 101 region, separated into sections focused on the local interstellar medium (Sect. 2), distance estimates (Sect. 3), the embedded young cluster (Sect. 4), and LkH α 101 itself (Sect. 5). We conclude with a brief preview of a new, comprehensive multiwavelength study of the region, and summarize the information with an eye toward future studies (Sect. 6).

2. The Interstellar Material

LkH α 101 is located just north of the Taurus-Auriga complex ($\alpha = 4^{\text{h}}30^{\text{m}}14.4^{\text{s}}$, $\delta = +35^{\circ}16'24''$ [J2000]; $l = 165.3^{\circ}$, $b = -9.0^{\circ}$) in the L1482 dark cloud. As Figure 1 demonstrates, the examination of an optical image near LkH α 101 reveals a complex



Figure 1. Optical *VRI* image of the NGC 1579 reflection nebula that hosts a young cluster surrounding LkH α 101 (from Herbig et al. 2004). The image is roughly 7 arcminutes on a side, with north up and east to the left.

local interstellar environment. The most prominent feature is a dark lane which cuts across the southeastern corner of the reddened reflection nebula NGC 1579 (discovered by William Herschel in 1788), illuminated by the apparently faint red source LkH α 101 near the image center. Redman et al. (1986) argue that this dark lane is in the foreground and probably not associated with LkH α 101. That argument is further supported by the interstellar H $_3^+$ chemistry constraints in the vicinity of an intense radiation source (Brittain et al. 2004). The reflection nebula was [mis]identified as the H II region S222 because of its redness in the Palomar survey plates (Sharpless 1959). However, subsequent observations showed that the polarization pattern from dust scattering was consistent with a reflection nebula entirely illuminated by LkH α 101 (Redman et al. 1986). A direct comparison of the optical spectrum of the nebula and LkH α 101 confirms this conclusion (Herbig, Andrews, & Dahm 2004). The evidence for an actual H II region is only inferred from the radio continuum spectrum (e.g., Brown, Broderick, & Knapp 1976; Dewdney & Roger 1986; Becker & White 1988): none of the optical or infrared lines typical of such physical conditions are present in the spectra of the nebula or LkH α

101 itself (Herbig et al. 2004). The latter probably could be explained if circumstellar material at high densities collisionally deexcites the standard forbidden emission lines.

Additional dark clouds to the north, south, and southwest were noted in coarse-resolution CO surveys of the region (Knapp et al. 1976; Redman et al. 1986; Barsony et al. 1990). The northern cloud is visible as a lip of material at the edge of the NGC 1579 nebula (see Fig. 1). Redman et al. (1986) present a schematic diagram of these various interstellar components (see their Fig. 8), and Herbig et al. (2004) discuss in some detail the small-scale structures in the medium immediately surrounding LkH α 101. Star counts and multicolor photometry (Barsony, Schombert, & Kis-Halas 1991) show that extinction is higher to the east of LkH α 101. In order of decreasing proximity to LkH α 101, the basic interstellar environment consists of: a dense circumstellar disk/envelope; a small H II region; a reflection nebula (NGC 1579); an HI envelope (Dewdney & Roger 1982); and a dark cloud (L1482) within a molecular filament.

LkH α 101 and its associated young cluster are embedded in this cloud filament, denoted TGU 1096 by Dobashi et al. (2005) and shown in Fig. 2, that extends northwest of the Taurus-Auriga complex ($d \approx 140$ pc; see the chapter in this volume by Kenyon, Gomez, & Whitney), and overlaps in projection with the more distant Per OB2 association ($d \approx 300$ pc; see the chapter in this volume by Bally et al.). Despite the apparent proximity of these two star-forming regions, the CO velocity of the filament is significantly different ($V_{\text{LSR}} = -1$ km s $^{-1}$) than for Tau-Aur (+6 km s $^{-1}$) and Per OB2 (+6-10 km s $^{-1}$; Ungerechts & Thaddeus 1987). Clearly this filamentary cloud and its contents are kinematically distinct from the Tau-Aur and Per OB2 clouds. Moreover, Herbig et al. (2004) note that the interstellar NaI absorption lines toward two stars in the young cluster are double, with core velocities consistent with those of Per OB2 and material in the filamentary cloud. As noted by those authors, this suggests that the interstellar material, embedded cluster, and LkH α 101 lie *beyond* the Per OB2 complex.

3. Distance Estimates

The sky-projected proximity of LkH α 101 to both the Tau-Aur and Perseus regions might be expected to create some confusion in estimating the distance to this star and its associated young cluster. Herbig (1971) originally estimated $d \approx 800$ pc based on spectra and UBV photometry of 2 early-type (B) stars near LkH α 101 that are associated with nebulosity. As discussed in Sect. 2, the interstellar medium signatures also appear consistent with a distance beyond the Perseus clouds ($d > 350$ pc; Ungerechts & Thaddeus 1987; Herbig et al. 2004). However, Stine & O'Neal (1998) argued that the radio luminosities of some cluster stars would be an order of magnitude larger than the mean for weak-lined T Tauri stars in Tau-Aur if the distance was as large as 800 pc. Given the location on the sky and this apparent radio luminosity discrepancy, Stine & O'Neal suggested a much smaller $d \approx 160$ pc. Using high resolution infrared measurements, Tuthill et al. (2002) identified both a companion star and a circumstellar disk around LkH α 101 (see Sect. 5). Given the proper motion of the companion and some model constraints on the star+disk mass, they find that $d \approx 200$ -500 pc can best explain the data, with a favored value $d \approx 340$ pc. Most recently, Herbig et al. (2004) extended the spectroscopic parallax measurements to 40 young cluster stars with a wide range of spectral types (from mid-M to early B) to estimate a larger distance, $d \approx 700$ pc.

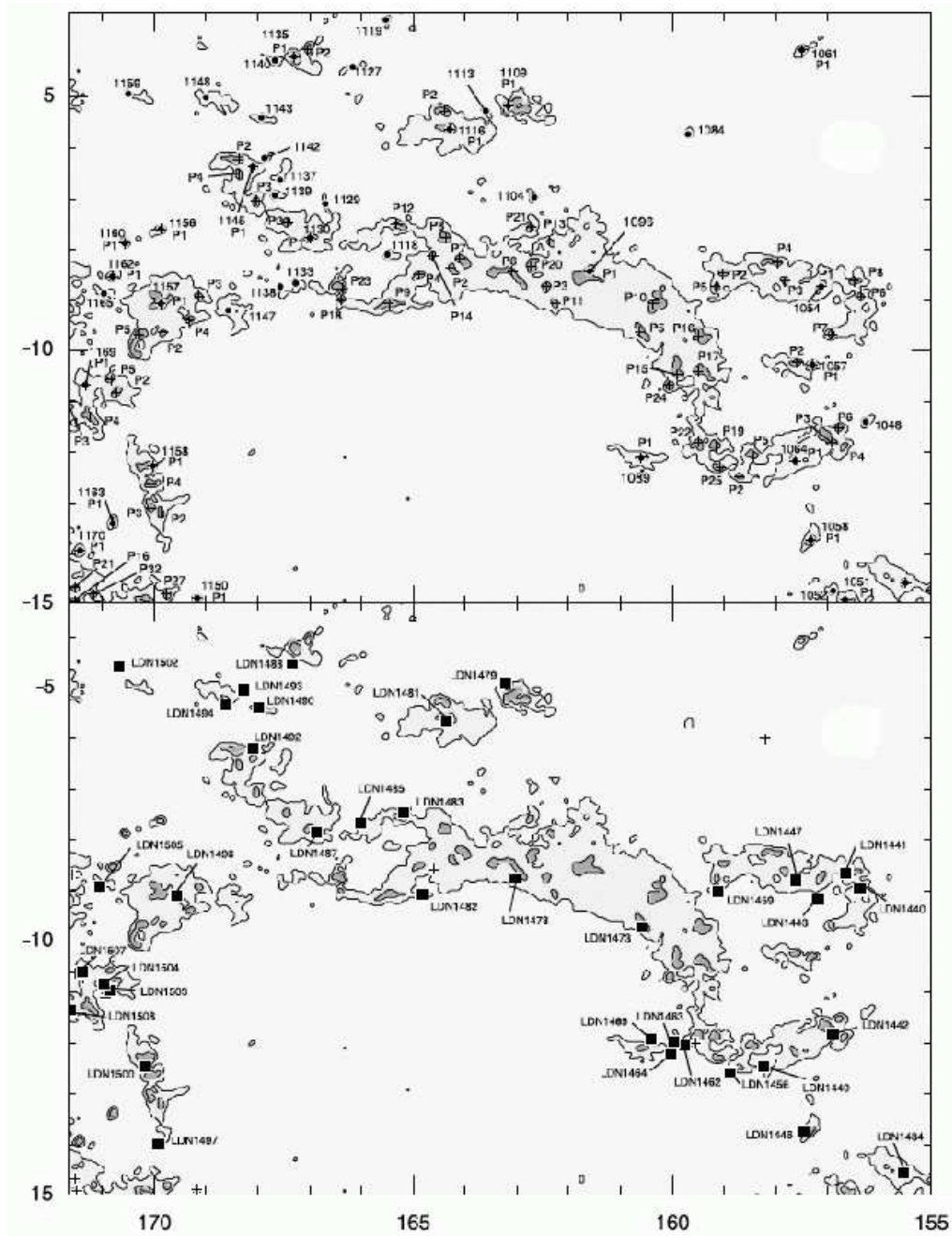


Figure 2. Extinction map of the large-scale region (TGU 1096) surrounding the L1482 dark cloud and the young cluster surrounding LkH α 101 embedded in it. The axes are galactic coordinates, and LkH α 101 is located at $l = 165.3^\circ$, $b = -9.0^\circ$.

Obviously, a definitive conclusion has yet to be reached. In the meantime, it would pay to consider the various pieces of observational evidence in a self-consistent man-

ner. Perhaps the most straight-forward distance estimate comes from the spectroscopic parallax determinations of cluster members. These measurements converge on a mean distance of 700 pc; and, although there is a scatter around this value of approximately ± 200 pc, there are no individual measurements consistent with a distance as low as 160 pc. We can turn to the H-R diagram for a consistency check on these values using the derived cluster age (see Sect. 4). Interstellar reddening uncertainties will not significantly affect the age determination because the reddening vector is roughly parallel to the isochrones. Therefore, the adopted distance acts to set the cluster age. As discussed further in Sect. 4, the cluster age is ~ 1 Myr for $d = 700$ pc. However, if the true distance were as close as $d = 160$ pc, the inferred cluster age would be ≥ 10 Myr, and therefore inconsistent with all the obvious indicators of youth that have been observed in the cluster (e.g., strong H α emission, infrared excesses, etc.).

Along with the above age-consistency argument and the evidence from the interstellar signatures (Sect. 2), Herbig et al. (2004) cautioned against adopting the $d \approx 160$ pc estimate advocated by Stine & O’Neal (1998) because only one of the four radio sources used by those authors is clearly associated with a weak-line T Tauri star. Further coupling this with the fact that none of the other 13 weak-line T Tauri stars in the LkH α 101 cluster were detected in the radio continuum, a comparison of the cluster radio luminosities with the Tau-Aur weak-line T Tauri star mean luminosity does not present a convincing argument for a small cluster distance. Instead, the preponderance of evidence suggests a large cluster distance, with most observational constraints in agreement with $d \approx 500$ -700 pc.

4. The Embedded Young Cluster

The first hints of an embedded young star cluster in this region came serendipitously from a radio study of the LkH α 101 stellar wind (Becker & White 1988). The radio map revealed a “necklace” of faint point sources surrounding the central star that in some cases appeared to be associated with optically detected low-mass stars. Those initial observations were revisited by Stine & O’Neal (1998), who identified more than a dozen compact sources, some of them exhibiting flaring gyrosynchrotron emission similar to those seen around weak-line T Tauri stars in Tau-Aur (e.g., Chiang, Phillips, & Lonsdale 1996).

Detailed multiwavelength observing campaigns were conducted soon after the radio discovery (Barsony et al. 1990, 1991), including broadband optical and infrared imaging, millimeter spectral line maps, and millimeter interferometry of the LkH α 101 circumstellar environment. Those studies first claimed a large infrared clustering of stars near LkH α 101, with an apparent age gradient indicating that the central star was quite young ($\sim 10^5$ yr). The latter conclusion remains somewhat an open question, due to the bright and spatially variable nebulosity in the vicinity of the hot star. These initial near-infrared images were then supplemented with *L*-band photometry to better determine the circumstellar properties of the stars in the cluster (Aspin & Barsony 1994). The color-color analysis in that study suggested that $\sim 30\%$ of the surveyed stars had excess thermal emission from the inner regions of circumstellar dust disks. This *L*-band excess fraction would be low for the apparent young age of the cluster (see below), according to the fairly well-established correlation noted by Haisch, Lada, & Lada (2001) and others. However, the completeness limit of these observations is difficult to estimate due to the bright infrared nebulosity in the region.

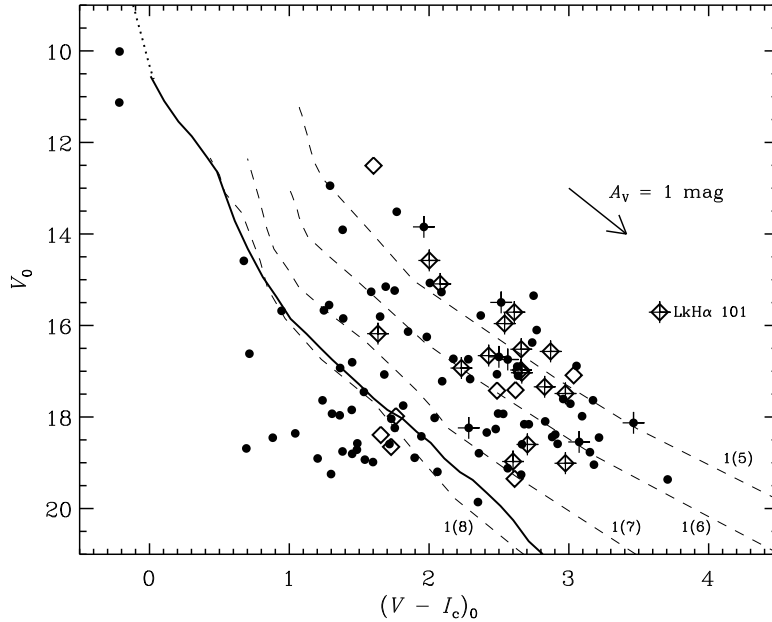


Figure 3. Color-magnitude diagram adapted from Herbig et al. (2004). The sources with known spectral types are marked with diamonds, and classical T Tauri stars with crosses. The solid line is the Pleiades main-sequence at $d = 700$ pc. The arrow shows the shift expected for an additional 1 magnitude of visual extinction. The dashed lines are theoretical isochrones from D’Antona & Mazzitelli (1997); ages are marked near the bottom of the figure.

More recently, Herbig et al. (2004) presented a comprehensive look at the embedded cluster and LkH α 101 itself using optical and infrared imaging and spectroscopy. Deep $BVRI$ imaging (see Fig. 1) enabled these authors to perform a standard analysis of the H-R diagram in an attempt to determine the cluster age. Figure 3 shows their reddening-corrected V , $V - I$ color-magnitude diagram for the cluster, along with some representative theoretical pre-main-sequence isochrones (D’Antona & Mazzitelli 1997). Supplementary spectroscopic data revealed 35 H α emission line stars (excluding LkH α 101) scattered around the cluster. Thirteen ($\sim 40\%$) of these H α emission line stars have equivalent widths less than 10 \AA (i.e., are weak-line T Tauri stars). The identifications of Herbig et al. (2004), celestial coordinates, representative optical and near-infrared magnitudes, and H α classifications (W = weak-line, C = classical T Tauri stars) are listed in Table 1 for reference.

Classification spectra for ~ 40 low-mass stars were compared with optical colors to infer a mean cluster distance of 700 pc and visual extinction of ~ 3.5 magnitudes. This spectroscopic parallax distance is in agreement with the earlier type stars in the cluster (see Herbig et al. 2004, their Fig. 6). Although a large spread in color-magnitude space exists within the cluster, the H α emission line stars (marked with crosses in Fig. 3) have a median age around 0.5 Myr using the aforementioned properties and isochrones.

In addition to these optical data, Herbig et al. (2004) obtained a deep ($K \leq 18.5$) set of JHK images of the region in an effort to search for the near-infrared excesses characteristic of the warm inner regions of circumstellar disks. A K -band mosaic image

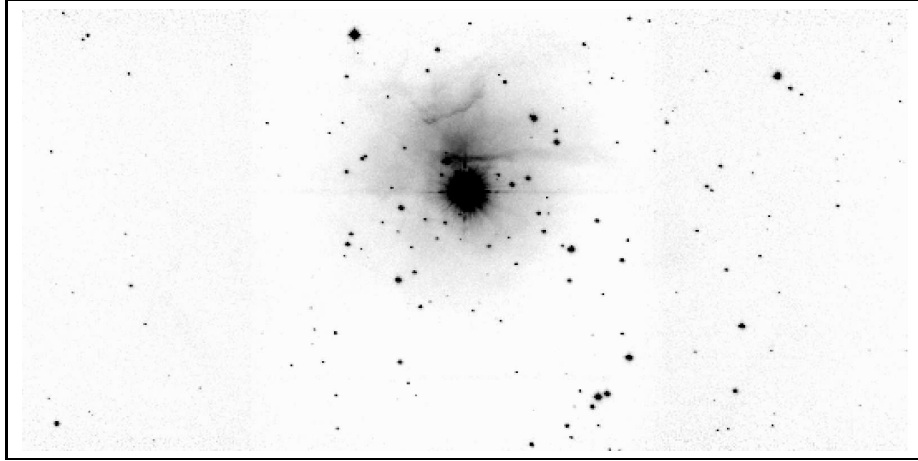


Figure 4. K -band image of the LkH α 101 cluster, covering 8' E-W and 4' N-S (from Herbig et al. 2004). The young star cluster is more apparent than in the optical (see Fig. 1), along with some interesting nebular features near the central source.

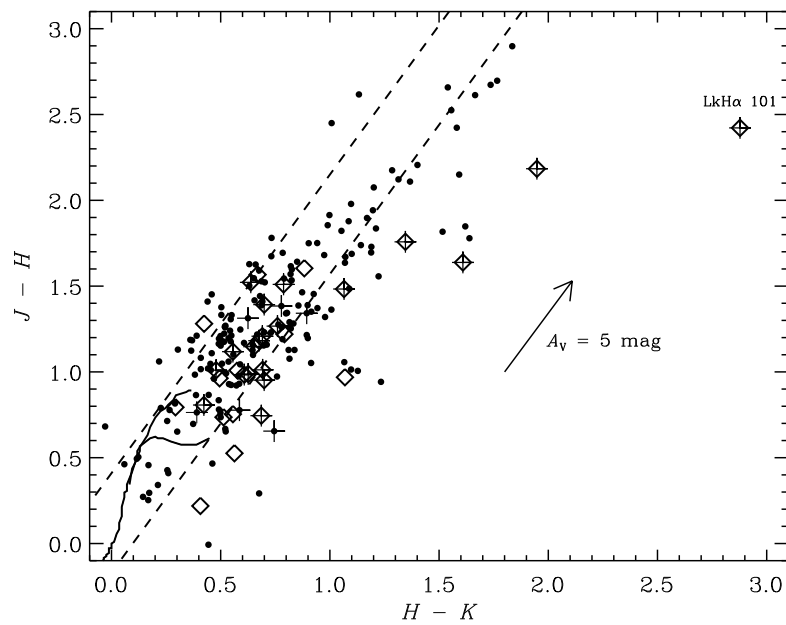


Figure 5. Near-infrared $J - H$, $H - K$ color-color diagram for the LkH α 101 cluster (from Herbig et al. 2004). The symbols are as in Figure 3. Solid curves mark normal main sequence and giant colors, and dashed lines define the reddening band.

Table 1. H α emission line stars near LkH α 101

# ^a	α [J2000]	δ [J2000]	R_c	K	H α ^b	excess ^c
10	04 29 56.35	+35 17 43.0	14.31	W	✓
27	04 29 58.61	+35 16 17.4	20.99	C
30	04 29 59.19	+35 18 48.6	21.80	C
32	04 29 59.72	+35 13 34.3	15.73	W
44	04 30 00.63	+35 17 18.4	18.08	11.40	W
63	04 30 02.21	+35 17 16.8	16.23	W
70	04 30 03.20	+35 14 21.5	21.69	13.33	W
72	04 30 03.58	+35 16 38.0	18.19	11.86	W
78	04 30 04.16	+35 16 27.5	20.10	11.98	C
83	04 30 04.62	+35 15 01.6	22.08	13.12	C	✓
95	04 30 05.89	+35 17 02.7	19.70	12.28	C	✓
100	04 30 06.65	+35 17 53.1	20.19	12.58	C
105	04 30 07.43	+35 14 58.6	16.71	C
107	04 30 07.50	+35 17 54.4	18.32	11.38	W
111	04 30 07.75	+35 15 49.0	18.38	11.18	C	✓
112	04 30 07.82	+35 14 09.7	17.84	11.77	C
118	04 30 08.36	+35 14 39.8	17.63	10.11	W
122	04 30 08.74	+35 14 38.3	17.15	C
126	04 30 08.97	+35 14 33.3	19.51	10.83	C
132	04 30 09.43	+35 17 41.0	20.33	12.05	C	✓
139	04 30 09.85	+35 14 17.1	19.83	12.57	C	✓
140	04 30 09.92	+35 15 54.7	18.85	10.61	C	✓
151	04 30 10.59	+35 16 56.2	18.81	C
157	04 30 11.08	+35 16 04.0	11.52	C	✓
180	04 30 13.05	+35 13 59.5	12.97	W
187	04 30 13.41	+35 18 11.4	18.09	W
192	04 30 14.26	+35 17 51.9	20.20	12.94	W	✓
194	04 30 14.44	+35 16 24.5	13.33	C
205	04 30 15.64	+35 17 38.4	21.18	10.94	C	✓
215	04 30 16.56	+35 15 42.7	19.40	11.59	C
225	04 30 17.24	+35 15 38.8	16.10	10.01	W
233	04 30 18.06	+35 18 18.8	20.75	W
243	04 30 19.35	+35 14 00.7	20.81	C
253	04 30 19.79	+35 14 21.9	20.07	12.79	C
303	04 30 30.41	+35 18 34.4	20.19	C
304	04 30 30.49	+35 17 45.5	20.07	11.80	C

^a Numbering system in machine-readable Table 1 of Herbig et al. (2004). LkH α 101 = 194.

^b H α emission line classification: W = weak line T Tauri star, C = classical T Tauri star.

^c A check mark notes the presence of emission in excess of the photosphere at 2.2 μ m.

of the region is shown in Figure 4. Using the near-infrared $J - H$, $H - K$ color-color diagram exhibited in Figure 5, these authors inferred that ~ 60 sources had an excess at 2.2 μ m; most of those are listed separately in Table 2, along with their positions and K -band magnitudes. Haisch, Lada, & Lada (2000) have pointed out, however, that excesses determined for such short wavelengths may not be representative of inner disk emission for a number of reasons: of particular concern here is the bright infrared nebulosity. Of these excess stars, 8 have $J - K > 4$ and 18 others have $3 \leq J -$

$K \leq 4$. This is in general agreement with the suggestions of Barsony et al. (1991) and Aspin & Barsony (1994) that an even younger, more embedded, population of stars may exist in the material surrounding LkH α 101.

Table 2. Near-infrared excess sources surrounding LkH α 101

# ^a	α [J2000]	δ [J2000]	K	# ^a	α [J2000]	δ [J2000]	K
6	04 29 55.82	+35 16 40.0	15.07	184	04 30 13.17	+35 16 33.6	15.32
22	04 29 58.25	+35 15 35.3	14.68	188	04 30 13.44	+35 15 41.5	14.98
34	04 29 59.94	+35 15 15.3	14.62	197	04 30 15.17	+35 15 30.6	15.24
46	04 30 00.76	+35 17 57.7	14.33	198	04 30 15.20	+35 16 40.4	10.17
50	04 30 01.24	+35 14 29.2	14.41	200	04 30 15.27	+35 16 33.3	12.28
82	04 30 04.59	+35 16 04.4	12.45	211	04 30 16.11	+35 16 10.0	12.50
89	04 30 05.52	+35 17 08.2	14.76	212	04 30 16.30	+35 15 24.7	11.86
117	04 30 08.24	+35 14 10.7	13.33	214	04 30 16.46	+35 14 38.9	14.40
133	04 30 09.51	+35 14 41.1	12.95	222	04 30 17.13	+35 16 16.3	10.38
141	04 30 09.97	+35 15 38.4	11.44	226	04 30 17.25	+35 16 03.8	13.20
150	04 30 10.57	+35 16 50.3	10.21	228	04 30 17.37	+35 15 21.4	15.93
154	04 30 10.89	+35 16 13.3	13.93	229	04 30 17.55	+35 16 26.6	13.31
155	04 30 10.94	+35 16 21.3	14.21	230	04 30 17.74	+35 17 13.7	13.38
167	04 30 11.76	+35 16 31.7	11.00	232	04 30 17.92	+35 16 08.4	13.24
168	04 30 12.19	+35 14 51.0	13.77	236	04 30 18.68	+35 16 42.9	12.46
170	04 30 12.23	+35 15 47.3	12.65	237	04 30 18.80	+35 16 41.9	11.88
173	04 30 12.34	+35 16 28.4	10.70	244	04 30 19.39	+35 15 57.3	10.92
175	04 30 12.77	+35 17 21.3	11.72	247	04 30 19.46	+35 16 34.9	11.80
178	04 30 13.01	+35 16 33.3	12.66	284	04 30 26.96	+35 14 49.0	15.53
181	04 30 13.08	+35 15 18.8	15.52	288	04 30 27.99	+35 15 15.7	13.80
182	04 30 13.09	+35 16 31.2	14.80	292	04 30 28.54	+35 15 51.1	15.71

^a Numbering system of Herbig et al. (2004).

5. LkH α 101

Since Herbig's (1956) identification of LkH α 101 as the illuminating source of the NGC 1579 reflection nebula, this still-enigmatic object has become one of the most thoroughly studied young stars in the sky. Early spectroscopic observations identified a remarkably strong H α emission line (equivalent width of ~ 550 Å; Herbig et al. 2004) and a series of other atomic emission features, dominated by permitted and forbidden lines of singly-ionized iron (Herbig 1956, 1971; Allen 1973; Thompson & Reid 1976). Assuming $d = 700$ pc, the position of LkH α 101 in an H-R diagram is consistent with an early B star (B0 or B1) on or near the main-sequence with a visual extinction of roughly 10 magnitudes (Herbig et al. 2004). Extinction estimates for the source vary significantly, but $A_V \approx 10$ lies comfortably in the center of the range of values. This spectral classification is in good agreement with that implied by the radio continuum observations, which require a Lyman continuum flux from a \sim B0.5 main-sequence star to explain the observed H II region emission (Harris 1976; Brown et al. 1976; Becker & White 1988; Hoare et al. 1994; Hoare & Garrington 1995). Despite these hints at the underlying radiation source, no stellar absorption features have ever

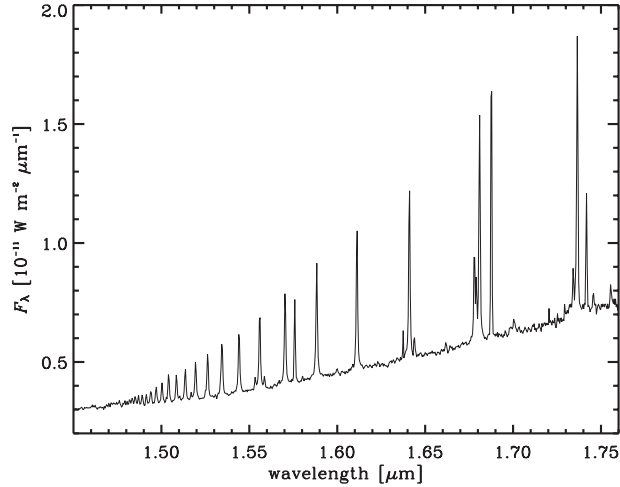


Figure 6. Portion of the near-infrared spectrum of LkH α 101 (taken with the SpeX instrument on the 3.0-m IRTF telescope). Brackett series lines can be seen to Br (42), in addition to some metal lines and a red continuum.

been clearly seen for LkH α 101 (Herbig et al. 2004). There is no *direct* spectroscopic evidence with which to classify the LkH α 101 photosphere.

Many of the spectroscopic studies of LkH α 101 have focused on understanding the physical conditions in the region(s) where the emission line spectrum is generated. In the near-infrared (1-5 μm), the spectrum is dominated by H I lines in the Paschen and Brackett series, along with various transitions of He I, Fe II, O I, and Mg II, among others (Thompson & Reid 1976; Thompson et al. 1976, 1977; Simon & Cassar 1984; Hamann & Persson 1989; Rudy et al. 1991). The optical spectrum has similar contributors (Hamann & Persson 1989; Kelly, Rieke, & Campbell 1994; Herbig et al. 2004). The oxygen and magnesium lines are thought to be excited by Bowen fluorescence from Ly β photons from the hot star (Hamann & Persson 1989). From this and the presence of high Paschen and Balmer series lines, some of which are shown in Figure 6, it is clear that the emission-line spectrum is at least partially generated in a high density, circumstellar environment.

Similar conclusions are reached based on forbidden emission line ratios (Kelly et al. 1994; Herbig et al. 2004) and the slope of the radio continuum (Brown et al. 1976). Hamann & Persson (1989) and Herbig et al. (2004) explored the possibility that electron scattering in such a dense circumstellar environment could broaden the standard early-type photospheric absorption lines into the continuum. The latter authors have ruled this out, and so the absence of these lines remains an unresolved issue. However, for photons to escape and produce the observed H II region, the star cannot be completely enveloped in such high-density material; the circumstellar emission line region must be geometrically anisotropic (e.g., Simon & Cassar 1984; Hamann & Persson 1989). These spectroscopic properties have led to comparisons of LkH α 101 and evolved massive stars which have moved off the main-sequence (e.g., η Car, MWC 300, MWC 349; Herbig 1971; Allen 1973; Thompson & Reid 1976; Hamann & Persson 1989). While acknowledging the very different evolutionary states of these objects and LkH α 101, the physical structures responsible for their similar

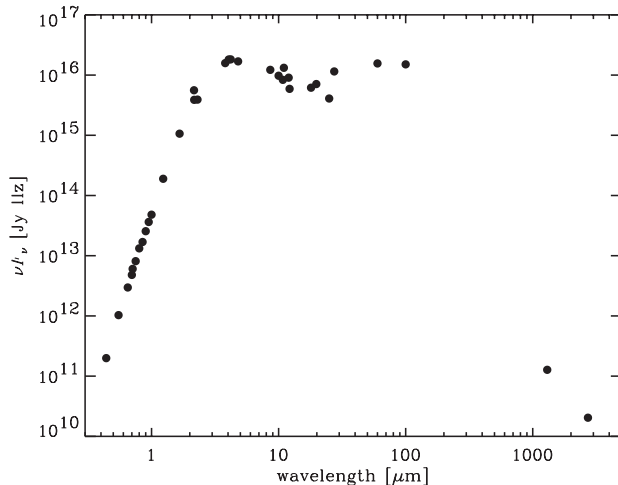


Figure 7. The broadband spectral energy distribution of LkH α 101, compiled from the literature (Cohen & Woolf 1971; Price & Murdock 1983; Simon & Cassar 1984; Barsony et al. 1990; Weaver & Jones 1992; Osterloh & Beckwith 1995; Danen, Gwinn, & Bloemhof 1995; Cutri et al. 2003; Herbig et al. 2004).

spectra are likely the same: stellar winds and the irradiation of a dense circumstellar disk.

The broadband spectral energy distribution (SED) of LkH α 101, displayed in Figure 7, shows a large infrared excess indicative of thermal continuum emission from circumstellar dust. Danen, Gwinn, & Bloemhof (1995) argued that the dip in the SED between ~ 10 and $20 \mu\text{m}$ is not easily explained by the standard circumstellar disk models (e.g., Adams, Lada, & Shu 1987; Beckwith et al. 1990). However, this is not likely a significant problem, as the large beam sizes for long-wavelength data often result in flux overestimates from extended emission or the excess emission from other nearby young stars in the cluster. Regardless, the $10 \mu\text{m}$ observations of Danen et al. indicated a very small emission source size ($\sim 50 \text{ mas}$) and warm characteristic dust temperature ($\sim 1000 \text{ K}$). Using the OVRO interferometer, Barsony et al. (1990) detected unresolved thermal continuum emission ($F_\nu \approx 185 \text{ mJy}$) at 3 mm from this circumstellar dust. With the standard optically thin, isothermal dust assumptions and opacity law (e.g., Andrews & Williams 2005), the corresponding mass of circumstellar material (gas and dust) is estimated to be $\sim 1\text{-}2 M_\odot$, or roughly 10% of the proposed stellar mass.

The remarkably bright infrared emission from LkH α 101 ($K \approx 3$) made it an ideal test subject for the rapidly developing technologies involved in very high-resolution infrared imaging. In a pioneering study by Tuthill, Monnier, & Danchi (2001), high angular resolution images showed that the infrared emission originates in a nearly face-on, resolved (FWHM = 40 mas) disk structure with a large central cavity surrounding the star. These and other data were shown to be consistent with high-mass disk models that call for an inner region cleared by the sublimation of dust particles by high-energy stellar irradiation and a thick, flared geometry (Tuthill et al. 2001, 2002). Moreover, these same data showed that the infrared emission morphology of the disk actually changes with time and revealed the presence (and relative proper motion) of a faint, blue companion star $\sim 0''.2$ to the northeast. Figure 8 shows a wider field H -band

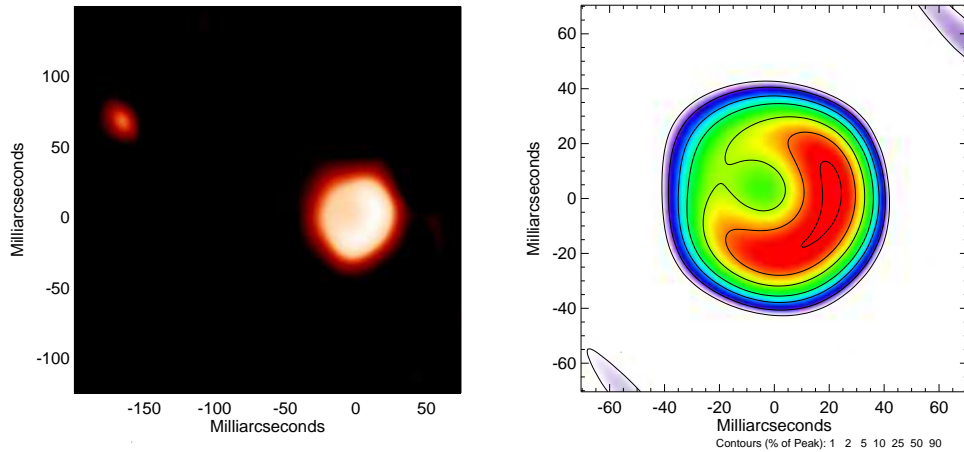


Figure 8. (*left*) High-resolution H -band image showing the bright disk around LkH α 101 and a faint companion star off to the northeast. (*right*) Detailed K -band image of the LkH α 101 disk, with a depressed central cavity and nearly face-on orientation. Images adapted from Tuthill et al. (2001, 2002), courtesy of P. Tuthill.

image with the LkH α 101 disk and this companion star, as well as a more detailed look at the disk morphology. Tuthill et al. (2002) used the motion of the companion star and properties of LkH α 101 and its disk to estimate an intermediate distance to the source, $d \approx 340$ pc. Herbig et al. (2004) noted that the disk geometry proposed by Tuthill et al. could account for the observed splitting of the optical Fe II lines, offering an interesting connection between the gas and dust in the inner disk.

6. Recent Results and Recommended Future Work

The embedded cluster around LkH α 101 has been the object of much recent scrutiny, as the subject of an infrared survey with the *Spitzer Space Telescope* and a simultaneous campaign with the *Chandra X-ray Observatory* and the VLA (Wolk et al. 2008; Osten & Wolk 2008). Images from the *Spitzer* and *Chandra* observations are shown together in Figure 9. The mid-infrared *Spitzer* photometry reveals the presence of 16 protostars (Class I sources) and an additional 95 T Tauri stars (Class II sources), along with 9 “transition” objects that show large $24 \mu\text{m}$ excesses but only photospheric emission at shorter wavelengths. The latter are widely interpreted to be circumstellar disks with evacuated inner regions. The *Chandra* observations identify an additional 65 X-ray sources coincident with infrared stars with near-photospheric colors, consistent with their association as more evolved (Class III) cluster members. This brings the total list of known cluster membership to ~ 185 , many of which are actively being confirmed spectroscopically (Winston et al. 2008).

In addition to identifying new members and characterizing their evolutionary states via their infrared excess properties, these new data can be utilized to estimate the total cluster size in two complementary ways. The first method exploits the empirical similarity of the X-ray luminosities from Class II and III sources (Feigelson & Montmerle 1999, and references therein). Using this assumption that the same fraction of Class II and III infrared sources should be detected with X-rays, the new observations imply

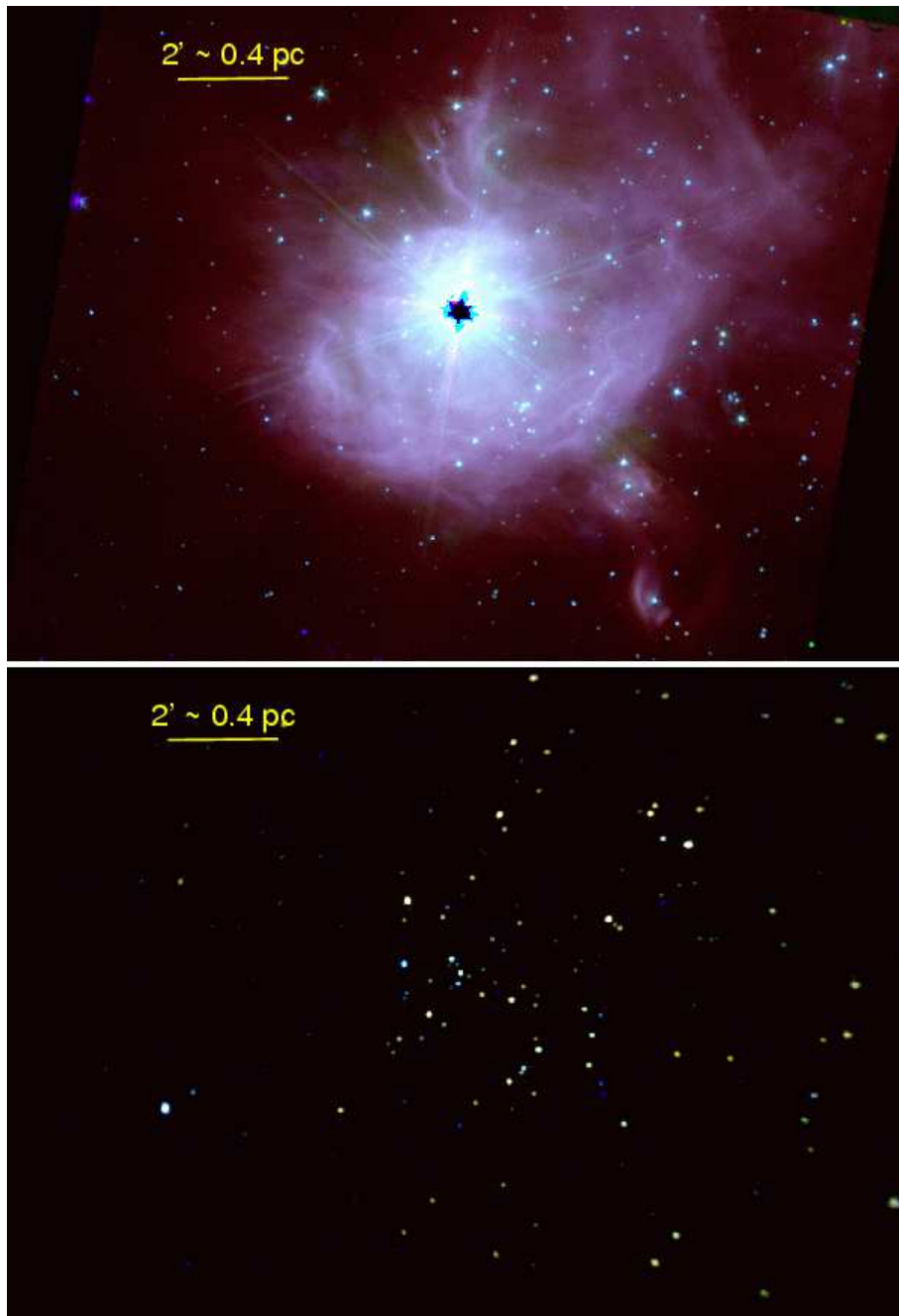


Figure 9. False color images of the LkH α 101 cluster at *Spitzer* mid-infrared (top) and *Chandra* X-ray (bottom) wavelengths (Wolk et al. 2008). The infrared image is a composite of data at 3.6 (blue), 4.5 (green), and 5.8 μm (red) on a logarithmic scale. The X-ray image is a composite of three energy ranges: 0.5-1.5 keV (red), 1.1-2.4 keV (green), and 2.1-8.0 keV (blue).

that the $\sim 45\%$ X-ray detection rate of Class II sources would translate to ~ 82 undetected Class III sources. This estimate would bring the total cluster membership to ~ 270 sources. The second method relies on the derived shape of the universal X-ray luminosity function (XLF) for young clusters asserted by Feigelson et al. (2005). If this universal XLF applies for the LkH α 101 cluster, the total cluster membership should be in the range of 280-330 stars, and the smaller cluster distances are firmly ruled out in favor of values in the range $d \approx 550\text{-}750$ pc. The closer end of this range brings the two methods of estimating cluster membership numbers into good agreement.

This recent work is encouraging in its focus on establishing a firm cluster membership base for future work. Only when a relatively complete membership roster has been obtained can a more comprehensive analysis of the distance, age, initial mass function, circumstellar disk fraction, and other basic properties be derived. Although of less immediate importance, a closer examination of individual cluster members would certainly be interesting. Herbig et al. (2004) present a curious high-resolution spectrum of the bright, nebulous star immediately to the northeast of LkH α 101 (their “Star D”, HBC 391; see Fig. 1), showing it to be an early K giant with a number of strange features. Those authors also note that none of the 5 B-type stars apparently associated with the same dark cloud (excluding LkH α 101) show the standard signatures of youth noted for other Herbig Be stars.

Given the high concentration of infrared sources in the immediate vicinity of LkH α 101 noted by Herbig et al. (2004), high angular resolution infrared images using adaptive optics would provide an interesting complement to the new *Spitzer* data. Some of the most interesting cluster members may be lurking in the tremendous glare of the central source, including the small group of stars identified by Herbig et al. (2004) that lie at one end of a “bar” of infrared nebulosity (see Fig. 4). Along these same lines, those interested in the formation and evolution of massive stars and their disks should make a concerted effort to follow up the high-resolution infrared work of Tuthill and colleagues. High resolution (sub-arcsecond) millimeter observations of the dust continuum and various molecular line transitions would aid tremendously in interpreting the circumstellar environment around LkH α 101. As with many other clusters in this book, the LkH α 101 region still holds a lot of promise for future observations with more sensitive, higher resolution instrumentation.

Acknowledgments. S.A. is very grateful to George Herbig and Scott Dahm for useful conversations and advice. We would like to thank Peter Tuthill for kindly providing the images in Figure 8.

References

- Adams, F. C. & Lada, C. J., ApJ, 312, 788
 Allen, D. A. 1973, MNRAS, 161, 1P
 Andrews, S. M. & Williams, J. P. 2005, ApJ, 631, 1134
 Aspin, C. & Barsony, M. 1994, A&A, 288, 849
 Barsony, M., Scoville, N. Z., Schombert, J. M., & Claussen, M. J. 1990, ApJ, 362, 674
 Barsony, M., Schombert, J. M., & Kis-Halas, K. 1991, ApJ, 379, 221
 Becker, R. H. & White, R. L. 1988, ApJ, 324, 893
 Beckwith, S. V. W., Sargent, A. I., Chini, R. S., & Güsten, R. 1990, AJ, 99, 924
 Brittain, S. D., Simon, T., Kulesa, C., & Rettig, T. W. 2004, ApJ, 606, 911
 Brown, R. L., Broderick, J. J., & Knapp, G. R. 1976, MNRAS, 175, 87P

- Chiang, E., Phillips, R. B., & Lonsdale, C. J. 1996, AJ, 111, 355
 Cohen, M. & Woolf, N. J. 1971, ApJ, 169, 543
 Cutri, R. M., et al. 2003, *2MASS All-Sky Catalog of Point Sources* (Pasadena: IPAC)
 Danen, R. M., Gwinn, C. R., & Bloemhof, E. E. 1995, ApJ, 447, 391
 D'Antona, F. & Mazzitelli, I. 1997, in *Cool Stars in Clusters and Associations*, ed. G. Micela & R. Pallavicini (Firenze: Soc. Astron. Italiana), 807
 Dewdney, P. E. & Roger, R. S. 1982, ApJ, 255, 564
 Dewdney, P. E. & Roger, R. S. 1986, ApJ, 307, 275
 Dobashi, K., et al. 2005, PASJ, 57, SP1, S1
 Feigelson, E. D., & Montmerle, T. 1999, ARA&A, 37, 363
 Feigelson, E. D., Getman, K., Townsley, L., Garmire, G., Preibisch, T., et al. 2005, ApJS, 160, 379
 Haisch, K. E., Lada, E. A., & Lada, C. J. 2000, AJ, 120, 1396
 Haisch, K. E., Lada, E. A., & Lada, C. J. 2001, ApJ, 553, L153
 Hamann, F., & Persson, S. E. 1989, ApJS, 71, 931
 Harris, S. 1976, MNRAS, 174, 601
 Herbig, G. H. 1956, PASP, 68, 353
 Herbig, G. H. 1971, ApJ, 169, 537
 Herbig, G. H., Andrews, S. M., & Dahm, S. E. 2004, AJ, 128, 1233
 Hoare, M. G., Drew, J. E., Muxlow, T. B., & Davis, R. J. 1994, ApJ, 421, L51
 Hoare, M. G., & Garrington, S. 1995, ApJ, 449, 874
 Kelly, D. M., Rieke, G. H., & Campbell, B. 1994, ApJ, 425, 231
 Knapp, G. R., Kuiper, T. B. H., Knapp, S. L., & Brown, R. L. 1976, ApJ, 206, 443
 Osten, R. A. & Wolk, S. J. 2008, ApJ, submitted
 Osterloh, M., & Beckwith, S. V. W. 1995, ApJ, 439, 288
 Price, S. D., & Murdock, T. L. 1983, *The Revised AFGL IR Survey Catalog and Supplement* (Air Force Geophys. Lab)
 Redman, R. O., Kuiper, T. B. H., Lorre, J. J., & Gunn, J. E. 1986, ApJ, 303, 300
 Rudy, R. J., Erwin, P., Rossano, G. S., & Puetter, R. C. 1991, ApJ, 383, 344
 Sharpless, S. 1959, ApJS, 4, 257
 Simon, M., & Cassar, L. 1984, ApJ, 283, 179
 Stine, P. C., & O'Neal, D. 1998, AJ, 116, 890
 Thompson, R. I., & Reid, M. 1976, 205, L159
 Thompson, R. I., Erickson, E. F., Witteborn, F. C., & Strecker, D. W. 1976, ApJ, 210, L31
 Thompson, R. I., Strittmatter, P. A., Erickson, E. F., Witteborn, F. C., & Strecker, D. W. 1977, ApJ, 218, 170
 Tuthill, P. G., Monnier, J. D., & Danchi, W. C. 2001, Nature, 409, 1012
 Tuthill, P. G., Monnier, J. D., Danchi, W. C., Hale, D. D. S., & Townes, C. H. 2002, ApJ, 577, 826
 Ungerechts, H., & Thaddeus, P. 1987, ApJS, 63, 645
 Weaver, W. B., & Jones, G. 1992, ApJS, 78, 239
 Winston, E. M., et al. 2008, ApJ, submitted
 Wolk, S. J., et al. 2008, ApJ, submitted